

Increased Colocalization and Interaction Between Decidual Protein Kinase A and Insulin-like Growth Factor–Binding Protein-I in Intrauterine Growth Restriction

Madhulika B. Gupta^{*}, Kyle K. Biggar, Cun Li, Peter W. Nathanielsz^{ID}, and Thomas Jansson^{*}

Department of Biochemistry and Department of Pediatrics, University of Western Ontario, London, ON, Canada (MBG); Children's Health Research Institute, London, ON, Canada (MBG); Institute of Biochemistry, Carleton University, Ottawa, ON, Canada (KKB); University of Wyoming, Laramie, Wyoming (CL, PWN); Southwest National Primate Research Center, San Antonio, Texas (TJ); and Division of Reproductive Sciences, Department of Obstetrics and Gynecology, University of Colorado Anschutz Medical Campus, Aurora, Colorado (TJ)

Summary

Increased phosphorylation of decidual insulin-like growth factor–binding protein-I (IGFBP-I) can contribute to intrauterine growth restriction (IUGR) by decreasing the bioavailability of insulin-like growth factor-I (IGF-I). However, the molecular mechanisms regulating IGFBP-I phosphorylation at the maternal–fetal interface are poorly understood. Protein kinase A (PKA) is required for normal decidualization. Consensus sequences for PKA are present in IGFBP-I. We hypothesized that the expression/interaction of PKA with decidual IGFBP-I is increased in IUGR. Parallel reaction monitoring-mass spectrometry (PRM-MS) identified multiple PKA peptides ($n > 30$) co-immunoprecipitating with IGFBP-I in decidualized primary human endometrial stromal cells (HESC). PRM-MS also detected active PKA^{Thr197} and greater site-specific IGFBP-I phosphorylation^{(pSer119), (pSer98+pSer101) (pSer169+pSer174)} in response to hypoxia. Hypoxia promoted colocalization [dual immunofluorescence (IF)] of PKA with IGFBP-I in decidualized HESC. Colocalization (IF) and interaction (proximity ligation assay) of PKA and IGFBP-I were increased in decidua collected from placenta of human IUGR pregnancies ($n=8$) compared with decidua from pregnancies with normal fetal growth. Similar changes were detected in decidual PKA/IGFBP-I using placenta from baboons subjected to maternal nutrient reduction (MNR) vs controls ($n=3$ each). In baboons, these effects were evident in MNR at gestational day 120 prior to IUGR onset. Increased PKA-mediated phosphorylation of decidual IGFBP-I may contribute to decreased IGF-I bioavailability in the maternal–fetal interface in IUGR. (J Histochem Cytochem 70. 515–530, 2022)

Keywords

fluorescent antibody technique, humans, hypoxia, mass spectrometry, maternal, nutrient reduction, papio, placenta, stromal cells

Introduction

Insulin-like growth factor-1 (IGF-1) is critical for normal placental and fetal development.¹ The biological activity of IGF-1 is strictly regulated by IGF-binding proteins. Specifically, when bound to its binding protein, IGF-1 cannot interact with its receptor, decreasing its bioavailability.² IGF-binding protein-1 (IGFBP-1),

Received for publication March 10, 2022; accepted June 10, 2022.

^{*}Equal contributions.

Corresponding Author:

Thomas Jansson, Division of Reproductive Sciences, Department of Obstetrics and Gynecology, University of Colorado Anschutz Medical Campus, Aurora, CO 80045, USA.
E-mail: thomas.jansson@cuanschutz.edu

predominantly synthesized by the basal plate decidua (BPD), is believed to be the most important IGF-binding protein in pregnancy.³ Importantly, the affinity with which IGFBP-1 binds IGF-1 is markedly increased when the IGFBP-1 is hyperphosphorylated.⁴ Interestingly, Westwood and co-workers reported that although IGF-2 is an equally important growth factor, phosphorylation of IGFBP-1 does not alter its affinity for binding IGF-1.⁵ Decidual IGFBP-1 regulates the bioavailability of IGF-1 within the local environment of the placenta.⁶ Increased decidual IGFBP-1 inhibits implantation and trophoblast invasion in intrauterine growth restriction (IUGR).⁷ However, the molecular mechanisms regulating decidual IGFBP-1 secretion and phosphorylation are poorly understood.

Casein kinase-2 (CK2) is known to phosphorylate IGFBP-1 in fetal liver and HepG2 cells.^{8,9} In addition, we reported activation of protein kinase C (PKC) in the phosphorylation of IGFBP-1 in HepG2 cells.¹⁰ We have also reported that human IUGR is associated with activation of decidual CK2 and increased site-specific phosphorylation of IGFBP-1 in the decidua and maternal circulation.¹¹ However, whether additional kinases mediate IGFBP-1 phosphorylation in the decidua is not well established. Frost and Tseng¹² have earlier proposed that stromal cell IGFBP-1 is a substrate for protein kinase A (PKA). Although the consensus kinase substrate sequence for PKA is present in IGFBP-1,¹³ PKA small interfering RNA (siRNA) silencing in HepG2 cells did not attenuate hepatic IGFBP-1 phosphorylation induced by leucine deprivation,¹³ raising the possibility that regulation of IGFBP-1 phosphorylation in decidua may differ from other tissues.

PKA is an essential kinase involved in major biological processes including gene expression, metabolism, cell growth, and cell proliferation.¹⁴ PKA is a major effector of the cAMP signaling pathway, which is essential for trophoblast fusion and therefore normal placental development.¹⁵ It is known that cAMP signal transduction cascade is activated during progesterone-dependent decidualization.¹⁶ Using endometrial stromal cells from rat uterus, it was suggested that the isozymes of cAMP-dependent PKA types I and II are both functionally important during decidualization.¹⁷

Although the direct causes of IUGR and the mechanisms underpinning IUGR remain poorly understood, limited fetal oxygen and nutrient availability is believed to be central to the pathophysiology of restricted fetal growth. Placental insufficiency, defined as a condition of impaired placental nutrient and oxygen transfer, is generally believed to originate in suboptimal trophoblast invasion in early pregnancy,^{18,19} often resulting in IUGR. Whereas IGFBP-1 can inhibit trophoblast

invasion²⁰ by sequestering IGF-1, the role of PKA in mediating hyperphosphorylation of decidual IGFBP-1 in IUGR remains unknown.

In vitro decidualized human immortalized endometrial stromal cells (HIESC) are an established model and widely used for the study of human decidual biology.^{21–23} HIESC show the phenotype of decidualized cells with extensive similarities to placental decidual cells.²⁴ We have previously reported IGFBP-1 hyperphosphorylation in response to hypoxia and nutritional deprivation in HIESC.²⁵

Nutrient and oxygen delivery from the placenta may also be compromised in maternal undernutrition. By feeding pregnant baboons a calorie-restricted diet (70% of controls),²⁶ our non-human primate model of maternal nutrient reduction (MNR) results in IUGR close to term. Although we have reported increased IGFBP-1 expression and phosphorylation in the liver of MNR baboon fetuses,^{8,27,28} the expression of decidual PKA and its association with IGFBP-1 in the baboon IUGR placenta have not been established.

Here, we applied targeted parallel reaction monitoring-mass spectrometry (PRM-MS), dual immunofluorescence (IF), and proximity ligation assay (PLA) approaches to determine PKA and IGFBP-1 interactions. We used fully decidualized primary human endometrial stromal cells (HESC)²⁹ and immortalized decidualized HESC [transformed HESC (T-HESC)]²² as in vitro models. In addition, we used human decidua from IUGR and healthy pregnancies with normal fetal growth and decidual samples from our non-human baboon model of IUGR due to MNR at GD120 and GD165 (full term GD185).²⁶ We hypothesized that the expression/interaction of PKA with decidual IGFBP-1 is increased in IUGR.

Methods

Isolation of Decidualized HESC and Hypoxia Treatment

These procedures were approved by Western University's Human Research Ethics Board (HERB) (# 114343). Placentas ($n=3$) were collected with informed consent at termination for non-medical reasons of uncomplicated 6- to 9-week pregnancies. Isolation and culture of primary HESC from termination placenta and details of in vitro decidualization have been reported previously.²⁹ In brief, cells were decidualized and serum starved overnight and subjected to either hypoxia (1% O₂) or normoxia (incubator air) for 72 hr. To achieve hypoxia, cells were placed in a hypoxic chamber (Billups-Rothenburg Inc.; San Diego, CA) which was flushed with 1% O₂, 5% CO₂, and balanced

N₂ gas mixture (Linde Canada Inc.; Mississauga, ON, Canada) for 15 min to ensure saturation.⁴ The cells in the sealed chamber were placed in a tissue culture incubator at 37C. Samples were collected after 72 hr of hypoxic treatment.

Parallel Reaction Monitoring-Mass Spectrometry

Immunoprecipitation of IGFBP-1. Equal aliquots of samples from in vitro decidualized HESC were used for PRM-MS analysis. Independent PRM-MS experiments ($n=4$) were performed using freshly extracted HESC from a pooled sample of $n=3$ placentas as described in detail previously.²⁹ In brief, decidualized primary HESC incubated under normoxia or hypoxia were immunoprecipitated (IP) with IGFBP-1 mouse monoclonal anti-human (mAb) 6303 antibody (Medix Biochemica; Kauniainen, Finland) using Protein A Sepharose beads (50 μ l, 50% slurry; GE Healthcare Bio Sciences AB, Uppsala, Sweden) as described previously.²⁹

PRM-MS Analyses of IGFBP-1 Peptides and PKA Autophosphorylation. The IP samples were digested in solution as described below for PRM-MS analysis. The quantification of site-specific phosphorylation of both IGFBP-1 and PKA was performed using PRM-MS approaches designed to monitor the presence of specific peptide mass (m/z) and peptides post-translationally modified at specific sites by phosphorylation. PKA peptides co-immunoprecipitated (co-IP) with IGFBP-1 were identified by PRM-MS and tested for its activation status.

For in-solution digestion of the IP samples, the sample was first digested using endoproteinase Asp-N incubated overnight at 37C (Roche Diagnostics Laval, QC, Canada), followed by digestion using trypsin (Roche Diagnostics) overnight at 37C. Peptide digests were desalted using C18-Zip Tip and dried. After desalting and drying, samples were loaded onto a Thermo Easy-Spray analytical C18 column (75 μ m i.d. \times 500 mm) with an Easy-nLC 1000 chromatography pump. For each analysis, we reconstituted peptides in 20 μ l of 0.1% trifluoroacetic acid (TFA) and loaded 4 μ l onto the column. Peptides were separated on a 125-min (5–40% acetonitrile) gradient. Mass spectra were collected on a Q-Exactive hybrid quadrupole-Orbitrap mass spectrometer coupled to an Easy-nLC 1000 system (Thermo-Fisher Scientific; London, Canada). The isolation list (Supplemental Table 1) with mass (m/z) and the sequences of the peptides used to identify IGFBP-1 by PRM-MS were developed and optimized using Skyline software. Each trace on the chromatograph (in color) represents the detection of each individual transition ion used to monitor phosphorylation. For both PKA and IGFBP-1, internal peptides were

used to normalize respective phosphopeptide data, and data were quantified using total peak area.

Cell Culture for Immunohistochemistry (IHC)

To perform IHC, we used HESC (ATCC CRL-4003) grown on poly-L-lysine glass coverslips with 75% confluency in six-well plates. The cells were decidualized using 1.0 μ M medroxyprogesterone acetate (MPA) (Pfizer Canada; Kirkland, Quebec) and 0.5 mM 8-bromo cAMP (Cayman Chemicals; Ann Arbor, MI), and decidualization was carried out for 6 days as described in detail previously.²⁴ For the hypoxia treatment, the decidualized HESC plates were placed in a hypoxic chamber and incubated with low oxygen tension (1% O₂, 5% CO₂, and 94% N₂) for 24 hr, whereas for normoxia cells were placed in normal incubator air (20% O₂, 5% CO₂, and 75% N₂ gas) and then in a 37C incubator on an orbital shaker for 24 hr. Next, the cells were fixed on coverslips with 4% paraformaldehyde for 1 hr at 4C, washed with PBS, and used for IHC.

Dual IF Analysis Using Decidualized HESC

Fixed decidualized HESC were encircled using a hydrophobic marker (ImmEdge PEN; Vector Laboratories, Inc., Burlingame, CA). Background Sniper (Biocare Medical, LLC; Pacheco, CA) was applied to each coverslip and incubated for 10 min in a humidity chamber. Cells were washed and primary antibodies were applied: anti-rabbit polyclonal IGFBP-1 (Kolling Institute of Medical Research) and anti-mouse monoclonal PKA (Santa Cruz Biotechnologies). The cells were incubated overnight at 4C. Following rinsing with PBS, secondary antibodies (Thermo-Fisher Scientific) were applied: Alexa Fluor 568 anti-rabbit (pseudo red) against IGFBP-1 and Alexa Fluor 488 anti-mouse (pseudo green) targeting PKA. Coverslips were incubated for 45 min at room temperature, followed by rinsing and counterstaining with 4',6-diamidino-2-phenylindole (DAPI) (Thermo-Fisher Scientific) and mounting onto slides using ProLong Diamond AntiFade Mounting Media (Thermo-Fisher Scientific).

Placental Collection

Human

Placentas were obtained from women at the London Health Sciences Centre (London, Ontario, Canada) with written informed consent approved by the Western University's Health Sciences Research Ethics Board (HSREB) (#102621). The set of samples used in this study are the same as we used in our previous studies^{11,30}; therefore, details of sample collection,

inclusion and exclusion criteria, and infant clinical data are as described previously.^{11,30} Placentas were collected from IUGR and appropriate for gestational age (AGA) pregnancies ($n=8$ in each group), and tissue containing decidua was fixed, embedded in paraffin, and subsequently sections ($5\ \mu\text{m}$) were prepared and stained with hematoxylin and eosin (H&E) to localize the BPD region.^{11,30} The selected AGA and IUGR sample blocks were serially cut so that each slide would include one of each sample type as schematically depicted previously.³⁰

Baboon

Details of housing and feeding regimens for baboons (*Papio cynocephalus hamadryas*, *Papio cynocephalus anubis*, and *Papio hamadryas anubis*) at the Southwest National Primate Research Center (San Antonio, TX, USA) have been provided previously.²⁶ All animal procedures were approved by the Texas Biomedical Research Institute Institutional Animal Care and Use Committee (no. 1134 PC). Following confirmation of pregnancy (at 30 days of gestation), the MNR regimen was initiated by feeding mothers 70% of total food (Purina Monkey Diet 5038) eaten by contemporaneous controls. Fetuses were delivered by cesarean section under general anesthesia and euthanized at gestational day (GD) 120 or GD165 (term ~185 days). Morphometric measurements were performed, placenta tissue was collected, and fixed baboon tissues were used as described for human tissues.

Dual IF in Human Placental Tissues

The protocol, reagents, and antibodies used for IF are all as described above for cells (HESC). In brief, fixed tissues from AGA and the GA-matched human IUGR tissue on the same slide were encircled with a hydrophobic pen. The tissues were treated using Biocare Background Sniper. For IF of fixed tissues, the following primary antibodies were used: anti-rabbit polyclonal IGFBP-1 (Kolling Institute of Medical Research) and anti-mouse monoclonal PKA (Santa Cruz Biotechnologies) singly or in combination. Secondary antibodies applied were Alexa Fluor 568 anti-rabbit (pseudo red) against IGFBP-1 and Alexa Fluor 660 anti-mouse (pseudo green) targeting PKA. The tissues were counterstained with the DAPI nuclear stain, and glass coverslips were mounted using ProLong Diamond AntiFade Mounting Media (ThermoFisher Scientific).

Imaging. Immunofluorescent images of single or dual-stained IF of HESC for randomized fields of view were imaged throughout the coverslips, to prevent and avoid

confirmation bias. IF for single or dual-stained cells, AGA and GA-matched IUGR (human) or control, and MNR (baboon) samples were captured under a Zeiss Axiolmager Z1 Microscope using Zeiss Zen Pro software (Carl Zeiss Canada Ltd.; North York, ON, Canada). These settings were consistent for all images taken so that this variable was controlled.

Images were generated at 10 \times , 20 \times , and 40 \times magnification, and multiple images were taken randomly from throughout the decidual region of the placenta for every tissue section to avoid confirmation bias. Under 10 \times and 20 \times imaging, some areas outside of the decidual region were included in the field of view. After images were taken, the images were visually analyzed and the IF of IGFBP-1 and PKA in GA-matched AGA and IUGR tissue sections was compared.

Proximity Ligation Assay (PLA)

PLA was performed on placental tissues from GA-matched human IUGR ($n=5$) and AGA pregnancies ($n=4$). Baboon placenta from GD120 (control and MNR $n=5$ each) and GD165 (control and MNR $n=3$ each) were run in parallel, by matching GD samples of control and MNR (IUGR) on the same slide. Following manufacturer's instructions, tissues were treated with Duolink blocking solution (Sigma-Aldrich) and then probed with a specific combination of primary antibodies for 1 hr at room temperature using polyclonal IGFBP-1 (Kolling Institute of Medical Research) and anti-mouse monoclonal PKA (Santa Cruz Biotechnologies). The PLA reaction was performed using the PLA secondary probes Duolink PLA Anti-Rabbit Plus and Anti-Mouse Minus diluted in Duolink antibody diluent (Sigma-Aldrich) and incubated for 1 hr. Subsequent ligation and amplification were performed using reagents and the manufacturer's instructions and as we described in detail previously.¹⁰ Coverslips were mounted (Sigma-Aldrich) in Duolink mounting media containing DAPI counterstain.

Image Standardization and Acquisition

Images from dual-stained HESC sections, placenta IF, or PLA were captured using an Axiolmager Z1 Epifluorescent Microscope and Zen Pro software (Carl Zeiss Canada Ltd.; Toronto, ON, Canada). After optimizing all acquisition parameters, representative 20 \times images were captured across the entire decidual area for each placenta, which subsequently provided an adequately large number of images ($n=12$) to minimize bias. For PLA imaging, z-stack images were captured and converted to extended depth-of-focus tagged image file format images to allow sharp visualization of all PLA spots. PLA-positive signal spots in AGA and

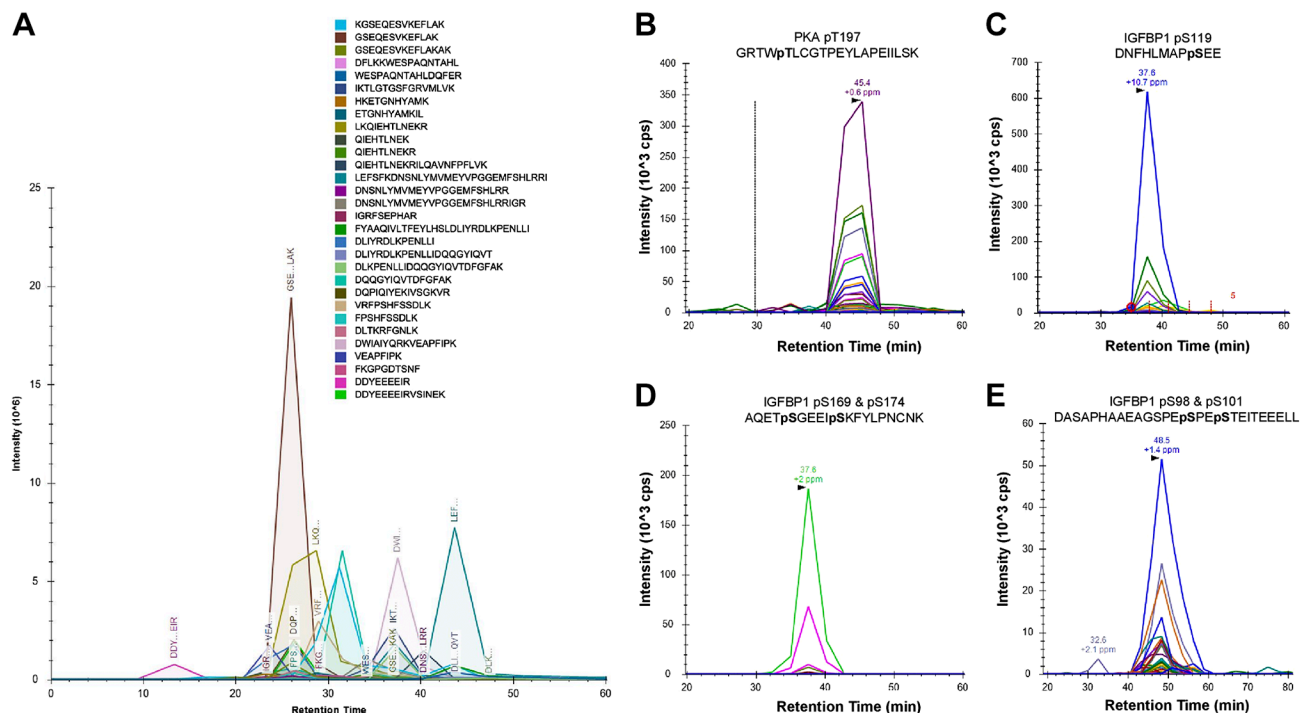


Figure 1. PRM-MS led to the identification of PKA-specific peptides from IGFBP-1 IP. Detection of PKA peptides by PRM-MS from IGFBP-1 immunoprecipitation (A). Chromatogram shows total transitions for 30 PKA-derived peptides; each peak monitors at least four daughter ions. Representative spectra of each daughter ion used to detect the presence of active PKC-pThr 197 from IP samples (B). Codetection of IGFBP-1 phosphorylated peptides (C–E). Chromatographs show transitions for four IGFBP-1 peptides, IGFBP-1-pSer119 (C), doubly phosphorylated IGFBP-1-pSer196 + pSer174 (D), and doubly phosphorylated IGFBP-1-pSer98 + pSer174 (E). All samples were doubly digested by trypsin and Asp-N protease and C18 cleaned prior to MS. Abbreviations: PRM-MS, parallel reaction monitoring-mass spectrometry; PKA, protein kinase A; IGFBP-1, insulin-like growth factor binding protein-1; IP, immunoprecipitation.

IUGR placental tissues were quantified using Image Pro Premier software (Media Cybernetics; Rockland MD) and normalized to the area of the decidual region of the placenta present in the images.

Data Presentation and Statistics

GraphPad Prism 5 (GraphPad Software Inc.; La Jolla, CA) was used for statistical analyses. Data presented are means \pm SEM. Unpaired *t* test was used to compare IUGR with AGA, or MNR and control, and $p < 0.05$ was considered significant.

Results

PRM-MS Analysis

To provide support for a functional interaction between decidual PKA and IGFBP-1, we performed IP of IGFBP-1 as in our recent study using primary decidualized HESC cultured in hypoxia or normoxia.²⁹ Using IP samples of decidualized primary HESC, we performed PRM-MS analysis to detect the presence and autophosphorylation status of PKA. PKA-specific

peptides from the IGFBP-1 immunoprecipitates collected from cultured decidual HESC samples were successfully detected (Fig. 1). In total, 30 PKA peptides were found to co-immunoprecipitate with IGFBP-1 (Fig. 1A; Supplemental Table 2). Furthermore, we also monitored the presence of auto-phosphorylated PKA at Thr197 (marker of increased PKA activity) (Fig. 1B) and IGFBP-1 phosphorylation at Ser119 (Fig. 1C), Ser169/Ser174 (Fig. 1D), and Ser98/Ser101 (Fig. 1E).

Next, we monitored the relative site-specific phosphorylation at each of these phosphorylation sites in hypoxia. In response to hypoxia, PKA was found to be co-IP with IGFBP-1 and phosphorylation of PKA at Thr197 (PKA activation) was increased by 3.6-fold compared with normoxic values (Fig. 2A). In addition, using the same IP samples, we found that IGFBP-1 phosphorylation increased in response to hypoxia. Specifically, IGFBP-1 phosphorylation at Ser119 increased 2.17-fold, doubly phosphorylated Ser98/pSer101 increased 1.92-fold, and doubly phosphorylated Ser169/pSer174 increased 5.63-fold when compared with normoxic levels (Fig. 2B). Collectively, these findings provide convincing evidence that PKA is a decidual kinase, resulting in enhanced protein-protein interactions with

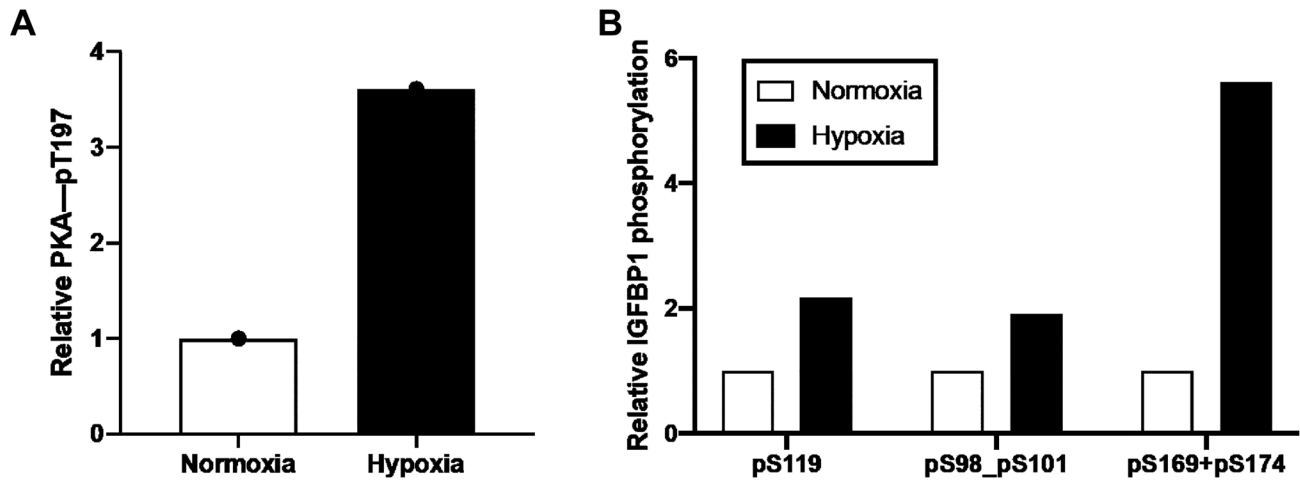


Figure 2. PRM-MS of relative PKA and IGFBP-1 phosphorylation in HESC samples in normoxic and hypoxic conditions. Active PKA autophosphorylation at Thr197 (A); IGFBP-1 phosphorylation at Ser119, Ser98+Ser101, and Ser169 + Ser174 (B). Relative values are determined from total peak intensities of transition ions from PRM-MS and normalized for protein abundance using internal peptide controls. Abbreviations: PRM-MS, parallel reaction monitoring-mass spectrometry; PKA, protein kinase A; IGFBP-1, insulin-like growth factor-binding protein-1; HESC, human endometrial stromal cells.

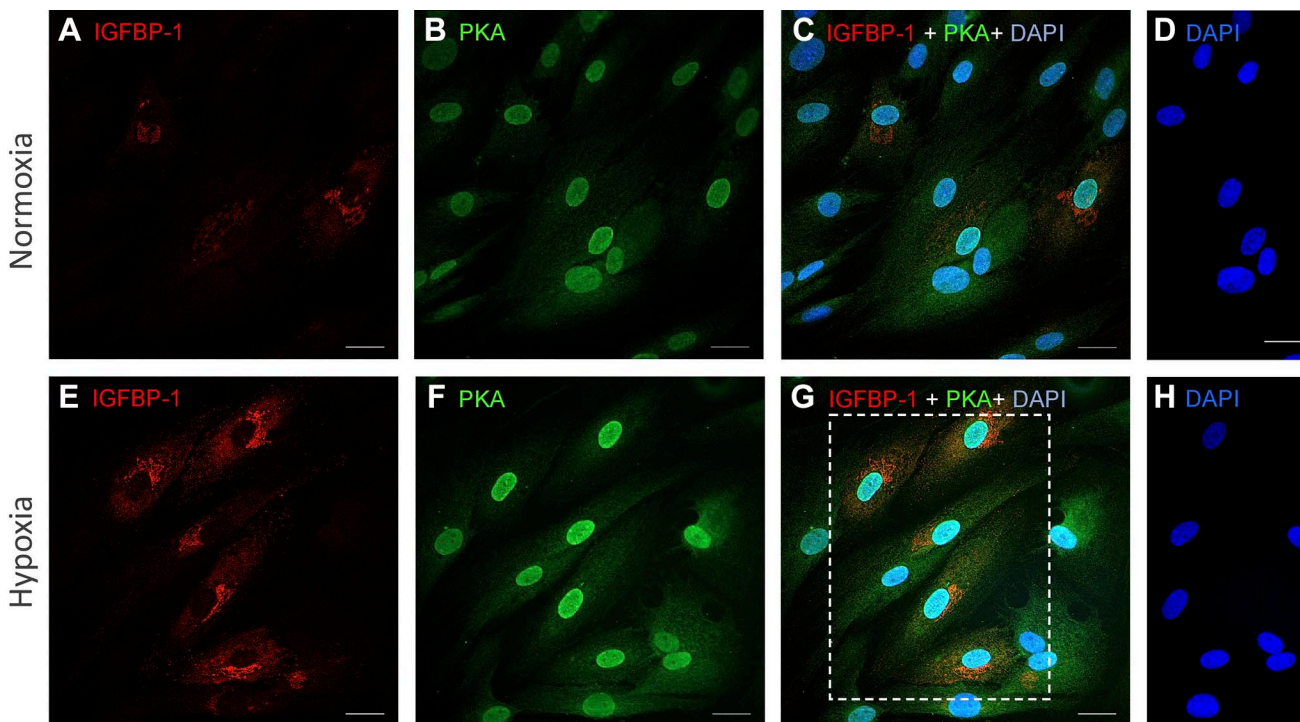


Figure 3. IGFBP-1 and PKA colocalization increases in decidualized T-HESC in response to hypoxia. Representative dual immunofluorescence staining of IGFBP-1 (red) (A, E) and protein kinase PKA (green) (B, F) in decidualized HESC cultured in normoxia or hypoxia. Merged confocal images depict colocalization between IGFBP-1 and PKA (red and green combined yield yellow) for normoxia and hypoxia (C, G). Nuclei are stained with DAPI (blue) (D, H). Scale bar = 25 μ m. Abbreviations: IGFBP-1, insulin-like growth factor-binding protein-1; PKA, protein kinase A; DAPI, 4',6-diamidino-2-phenylindole; HESC, transformed human endometrial stromal cells.

IGFBP-1 in hypoxia. Furthermore, IP with rabbit preimmune IgG used as a negative control failed to immunoprecipitate IGFBP-1. PRM-MS data provide strong evidence that the PKA interacts with IGFBP-1 in primary decidualized HESC.

IGFBP-1 and PKA Colocalization Increases in Decidualized HESC in Response to Hypoxia

Dual IF imaging of HESC (Fig. 3A–H) revealed that the expression of IGFBP-1 (Fig. 3E) and PKA (Fig. 3F)

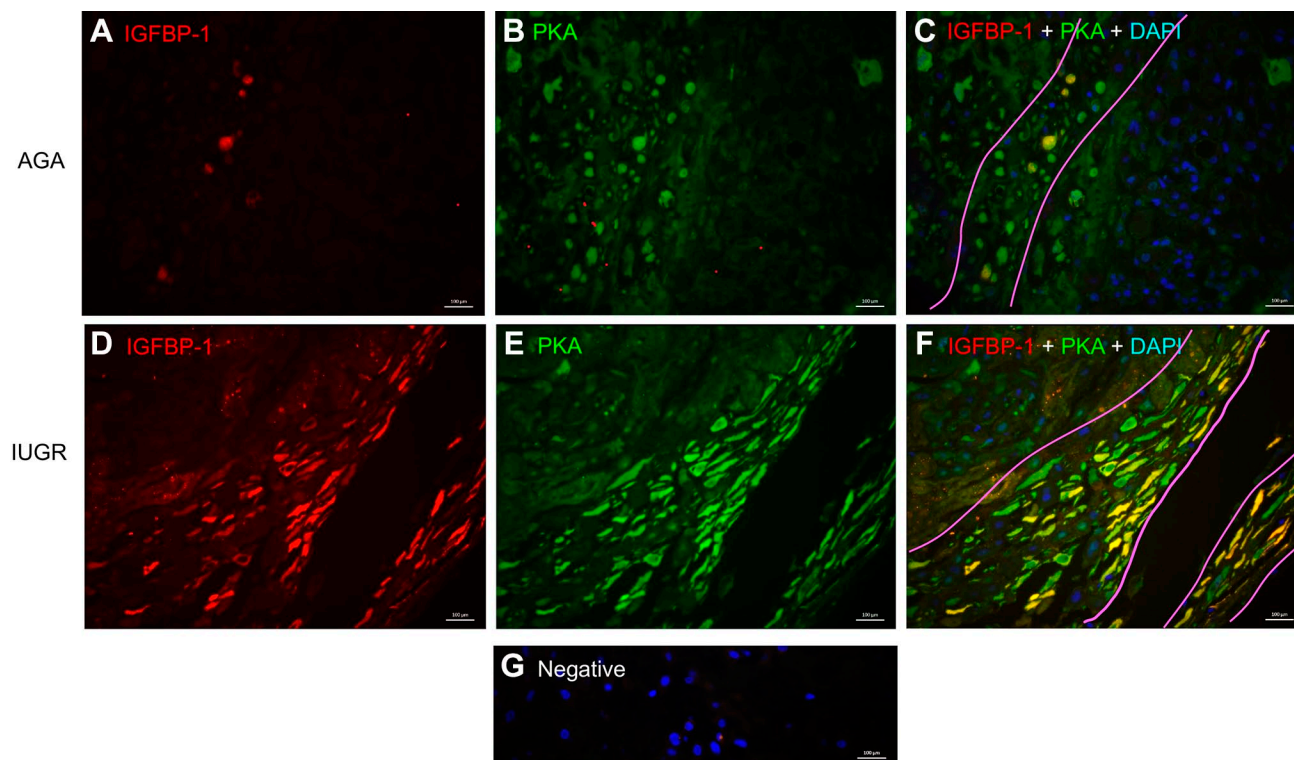


Figure 4. Increased colocalization of decidual IGFBP-1 and PKA in term human IUGR placenta. Representative immunofluorescence images of IGFBP-1 (Alexa 568, red) and protein kinase A (Alexa 660, green) are shown in AGA and from the GA-matched IUGR placenta. Images were captured across the entire decidual area for each placenta, which subsequently provided an adequately large number of images ($n=12$) to minimize bias. Both IGFBP-1 (red) and PKA (green) signals along with single channel images (A–D) are shown with increased signals in the decidual region of the placenta. Merged multichannel images indicate colocalized signal (C–F). Nuclei are stained with DAPI (blue) (A–B); negative control (G). Original scale bars, 20 μ M. Abbreviations: IGFBP-1, insulin-like growth factor-binding protein-1; PKA, protein kinase A; IUGR, intrauterine growth restriction; DAPI, 4',6-diamidino-2-phenylindole; GA, gestational age; AGA, appropriate for gestational age.

increased in response to hypoxia compared with normoxia (Fig. 3A and B). Importantly, dual staining showed a clear, yellow-orange overlap mainly in hypoxia (Fig. 3G) (shown within dotted box), suggesting that IGFBP-1 and PKA were colocalized (Fig. 3C and G). This finding is consistent with PRM-MS using primary decidualized HESC, demonstrating both increased PKA and IGFBP-1 expression in hypoxia (Fig 2A and B), providing further evidence for potential interaction between PKA and IGFBP-1.

Increased Colocalization of Decidual IGFBP-1 and PKA in Human IUGR Placenta

Clinical information of the same study subjects ($n=8$ each, AGA and IUGR) has been provided previously¹¹ where we reported there were no significant differences in maternal age, maternal height, or gestational age between groups. Birth weights of IUGR babies were 57% lower than the birth weights of AGA babies

($p=0.0002$), and the IUGR placental weights were significantly lower than the AGA placental weights ($p=0.0046$). Umbilical artery ($p=0.0366$) and venous pO_2 ($p=0.0192$) were lower in IUGR compared with AGA, consistent with fetal hypoxemia and with placental insufficiency.

Dual Immunofluorescence. Dual IF imaging of placenta (Fig. 4A–F) shows that IGFBP-1 (pseudo red) was predominantly localized in the decidual region (right side of tissue; Fig. 4A and D), whereas PKA (pseudo green) appeared to be widely expressed also in cells outside the decidual region, including possibly in the trophoblast and endothelial cells of chorionic villi (left side of the image; Fig. 4B and E), but with higher expression evident in the decidual region. Importantly, dual staining shows a clear, yellow overlap mainly in IUGR (Fig. 4F), with both IGFBP-1 and PKA in decidual regions revealing considerable colocalization, which markedly increased in IUGR (Fig. 4F)

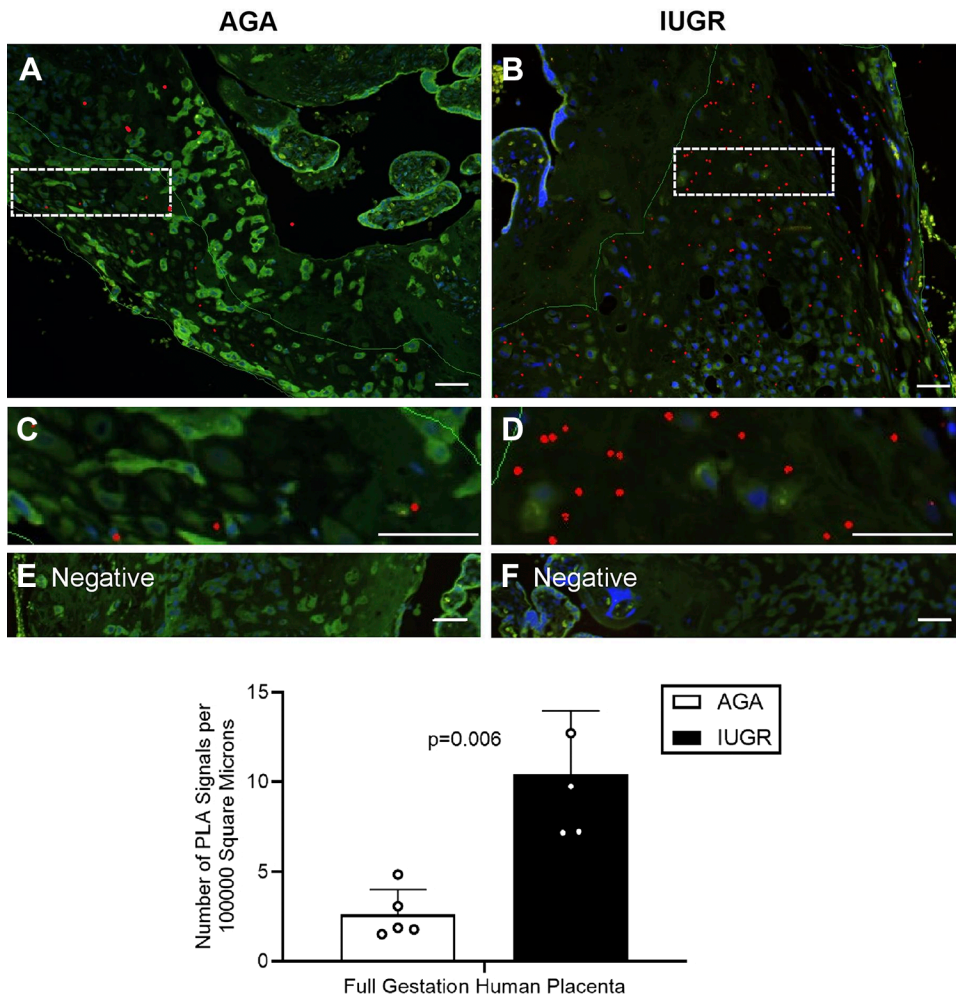


Figure 5. Increased colocalization of decidual IGFBP-1 and PKA in term human IUGR placenta as demonstrated by PLA. Representative PLA signals in images of IGFBP-1 and PKA in the decidual region of human placenta (indicated by the red dots) demonstrate the potential interaction in IUGR compared with AGA. Cropped and zoomed-in images (C–D) correspond to the white-dashed boxes in (A–B). Nuclei are stained with DAPI (blue). Negative controls (E–F). Bar graph indicates an increase in PLA signals in IUGR compared with AGA ($p=0.006$). Original scale bars, 50 μm . Abbreviations: IGFBP-1, insulin-like growth factor-binding protein-1; PKA, protein kinase A; IUGR, intrauterine growth restriction; PLA, proximity ligation assay; DAPI, 4',6-diamidino-2-phenylindole; AGA, appropriate for gestational age.

compared with AGA (Fig. 4C). Negative control in the absence of primary antibodies depicted no nonspecific staining (Fig. 4G).

Proximity Ligation Assay. The potential interaction of PKA and IGFBP-1 was further investigated in IUGR and gestational age-matched AGA human placenta using PLA (Fig. 5). Positive signals appear as red spots [enhanced for visual assessment, box with dotted line (Fig. 5A and B)] and are shown zoomed (Fig. 5C and D). Z-stack extended-focus imaging and Image-Pro Premier software were used to demonstrate PLA interactions through PLA spot counting. A 4-fold increase in the number of PLA spots was detected in IUGR (Fig. 5D) vs AGA (Fig. 5C) shown in histogram (Fig. 5G)

($p=0.006$). This suggests that PKA and IGFBP-1 are very closely (at distances <40 nm) localized, and that there is a potential for interaction between these proteins in decidua. PLA signals were not visible in the absence of primary antibodies (Fig. 5E and F).

Increased Colocalization of Decidual IGFBP-1 and PKA in MNR Baboons

Baboon Samples. Morphometric measures from MNR and control baboons at GD120 and GD165 are published in our previous papers.^{8,27,28} MNR did not affect fetal weight at GD120 but reduced fetal weight at GD165 (-13% , $p=0.030$). Similarly, relative fetal liver weight was unaffected at GD120, but was reduced at

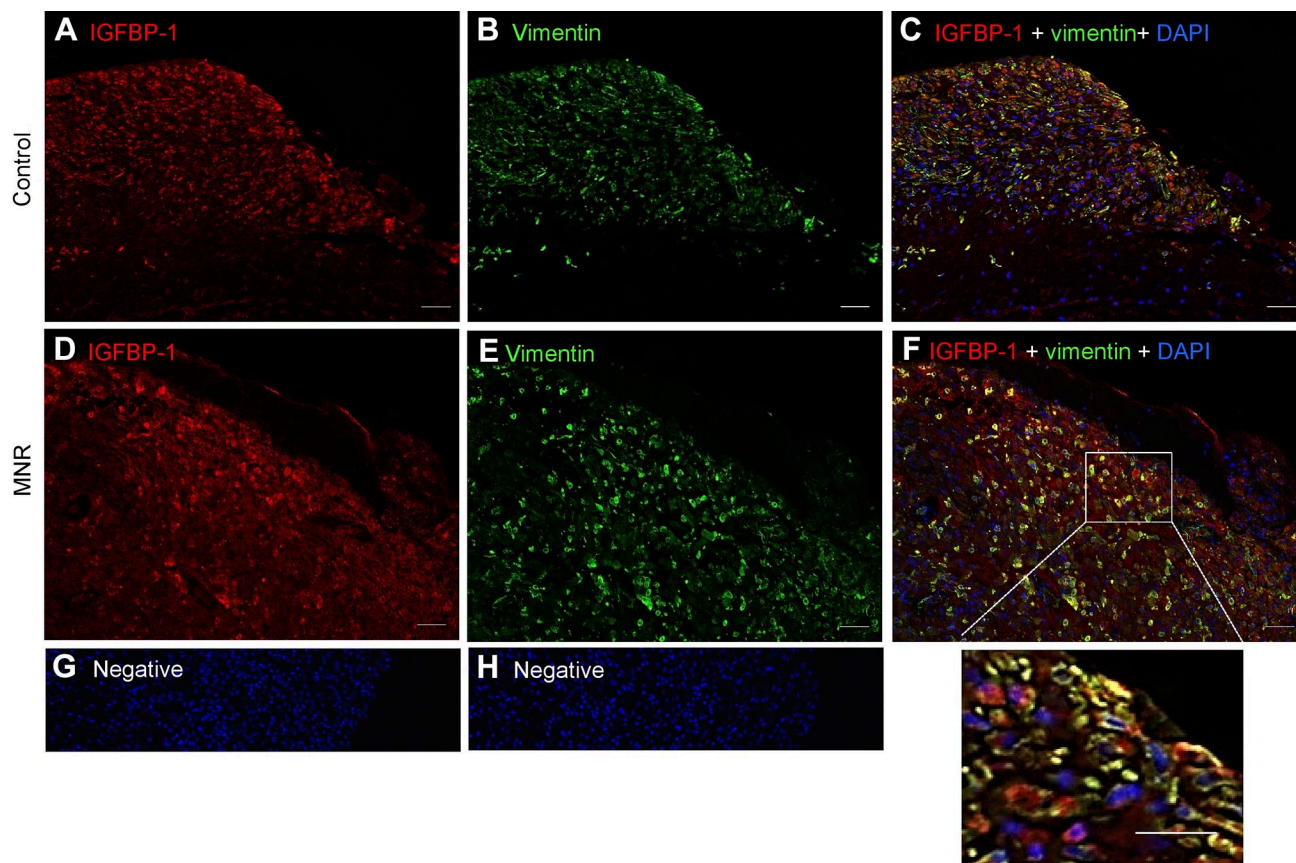


Figure 6. Increased decidual IGFBP-1 and vimentin colocalization in MNR baboons at gestational day 120. Representative immunofluorescence staining of IGFBP-1 (green) and vimentin (red) is shown in control and MNR baboon placenta at gestational day 120. Decidual region shows increased colocalization of IGFBP-1 and vimentin (indicated in yellow) in MNR (F) compared with control (C) in merged channels. Negative controls (G and H). Nuclei are stained with DAPI (blue). Abbreviations: IGFBP-1, insulin-like growth factor binding protein-1; MNR, maternal nutrient reduction; DAPI, 4',6-diamidino-2-phenylindole; IUGR, intrauterine growth restriction; PLA, proximity ligation assay; AGA, appropriate for gestational age.

GD165 by 9% ($p=.047$). These changes reflect the onset of IUGR by GD165. The concentrations of some key essential amino acids, such as leucine, isoleucine, and phenylalanine, were decreased in fetal cord plasma at GD120 and GD165 in MNR animals, consistent with reduced nutrient availability.²⁶

Increased Decidual IGFBP-1 and Vimentin Colocalization in MNR Baboons at GD120 and GD165. Literature suggests vimentin highlights predominantly mesenchymal cells,³¹ whereas IGFBP-1 is known to be strongly expressed mainly in decidualized cells as we reported in our previous study.³⁰ Using vimentin as a marker for mesenchymal cells/stromal decida, we first defined the mesenchymal cell types of the baboon placenta in MNR and control tissue ($n=3$ each). Dual IF images with IGFBP-1 (red) and vimentin (green) on GD-matched baboon MNR are shown at GD120 (Fig. 6) and GD165 (Fig. 7), where vimentin-positive staining was clearly present in mesenchymal cells/

stromal decidual cells. The decidual cells were strongly immunoreactive for both vimentin (Fig. 6B and E) and IGFBP-1 (Fig. 6A and D). Dual IF patterns showed an increase in IGFBP-1 expression in vimentin-positive decidual cells in baboon MNR at GD120 (Fig. 6F), prior to a decrease in fetal weight. At GD165, when IUGR is observable,²⁶ findings were similar (Fig. 7F).

Increased Decidual IGFBP-1 and PKA Colocalization in MNR Baboons at GD120. Dual IF showed that IGFBP-1 expression and its colocalization with PKA in baboon MNR placentas was increased at GD120 (Fig. 8C and F). To confirm colocalization from our widefield imaging was real and not due to technical artifact, we performed two-dimensional deconvolution of images (Fig. 9C and F) using NIS Elements software (Nikon Instruments Inc; Melville, NY) and the automatic deconvolution algorithm. Deconvolution relocates the scattered fluorescent signals (potentially evident as an artifact of widefield imaging) back to their point source

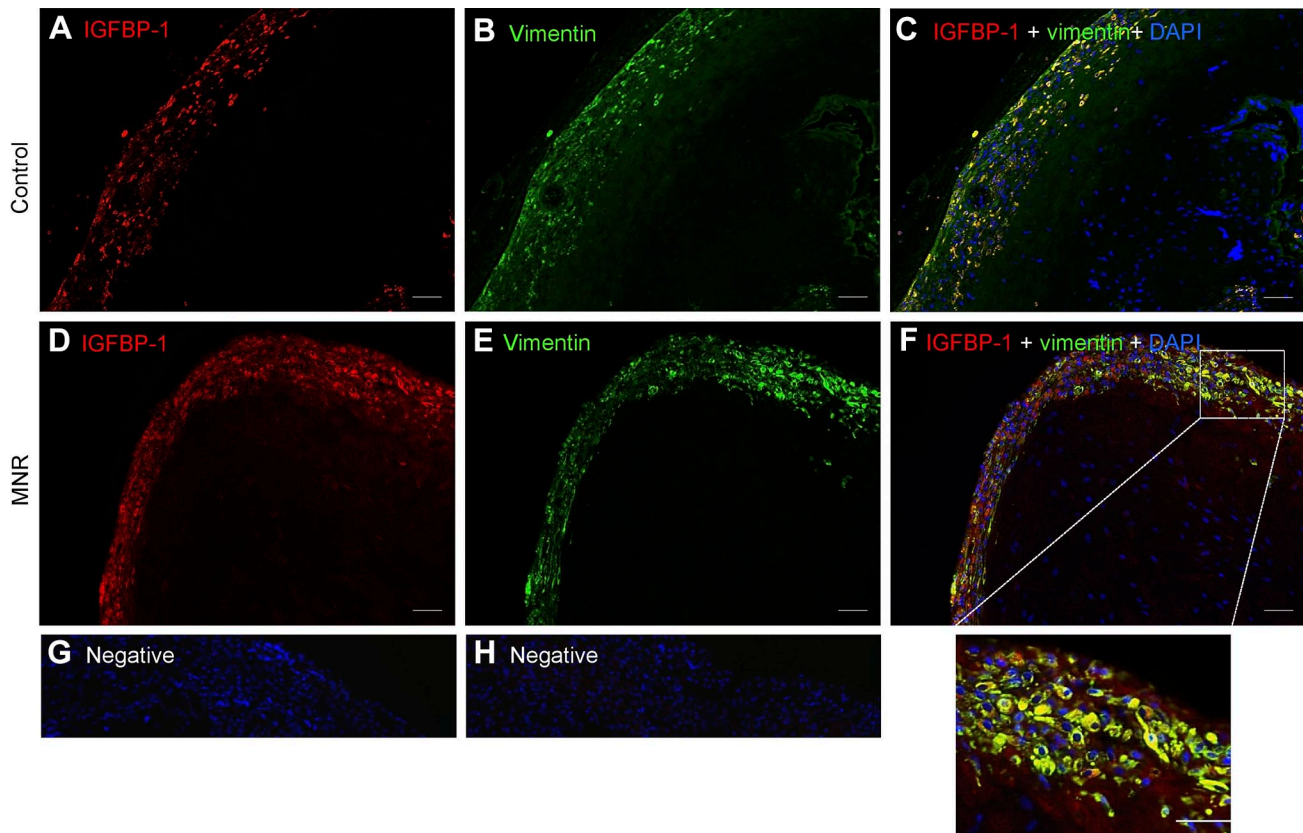


Figure 7. Increased decidual IGFBP-1 and vimentin colocalization in MNR baboons at gestational day 165. Representative immunofluorescence staining of IGFBP-1 (green) and vimentin (red) in control and MNR baboon placenta at gestational day 165. Decidual region shows increased colocalization of IGFBP-1 and vimentin (indicated in yellow) in MNR placenta (F) compared with control (C) in merged channel images. Negative controls (G and H). Original scale bars, 50 μ m. Abbreviations: IGFBP-1, insulin-like growth factor binding protein-1; MNR, maternal nutrient reduction; DAPI, 4',6-diamidino-2-phenylindole.

so that any yellow (red + green) pixels after deconvolution can only be detected from truly colocalized signals. Single-channel IGFBP-1 (Fig. 9A and D) and PKA (Fig. 9B and E) are shown as multichannel, deconvolved images (Fig. 9C and F). These data revealed strongly colocalized pixels (zoomed figure insets, Fig. 9C and F), which confirmed the colocalization of IGFBP-1 and PKA in the decidua of both control and MNR baboons. We found marked increase in areas of colocalization in the MNR decidua (Fig. 9F), further suggesting an interaction between these proteins. Increase in decidual IGFBP-1 and PKA colocalization in MNR baboons was also observed at GD165 (Fig. 10C and G).

Increased Colocalization of Decidual IGFBP-1 and PKA in MNR Baboons at GD120 and GD165 as Demonstrated by PLA. The potential interaction of PKA and IGFBP-1 in MNR baboon decidua was determined using PLA (Fig. 11). For enhanced visual assessment, dotted boxes at GD120 are shown zoomed (Fig. 11C and D) and at GD165 (Fig. 11I and J), spots are artificially enlarged.

We observed increased PLA-positive signals for PKA and IGFBP-1 in MNR (Fig. 11D) compared with AGA (Fig. 11C) at GD120 and similarly at GD165 (Fig. 11I and J). Z-stack extended-depth-of-focus imaging and Image-Pro Premier software were used to demonstrate PLA interactions through PLA spot counting. Significantly greater number of PLA spots (red) were detected in MNR as shown in histogram (Fig. 11M) compared with AGA ($p=0.002$) at GD120 and at GD165 vs AGA ($p=0.003$), representing close proximity between IGFBP-1 and PKA both at GD120 and at GD165.

No PLA interactions were visible in the absence of primary antibodies (Fig. 11E, F, K, and L). PLA data were highly consistent with IHC and suggest the potential for greater IGFBP-1 phosphorylation in MNR due to increased IGFBP-1 and PKA interaction, which remained consistent at both GD120 and GD165.

Discussion

In the current study, we provide novel evidence that PKA may be another key kinase involved in

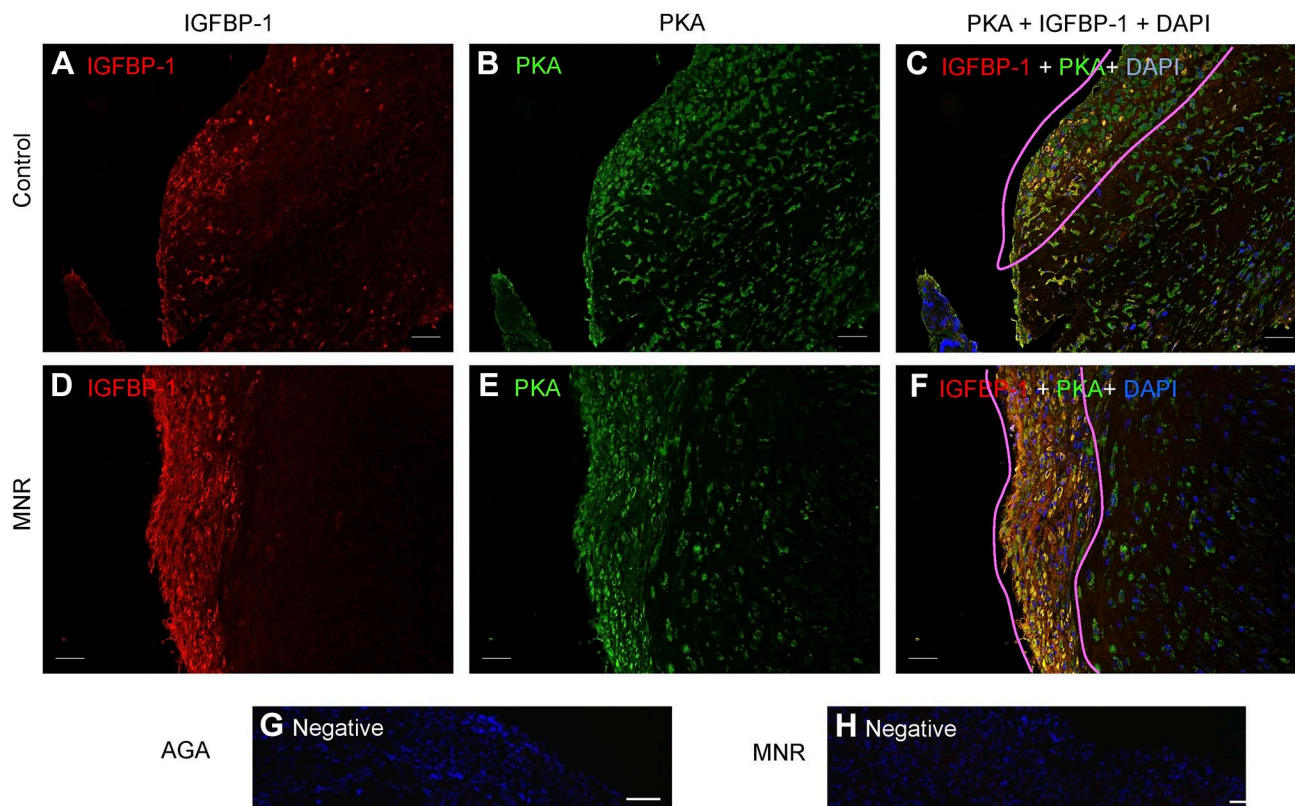


Figure 8. Increased decidual IGFBP-1 and PKA colocalization in MNR baboons at gestational day 120. Representative dual immunofluorescence staining of PKA (green) and IGFBP-1 (red) in control and MNR baboon placenta at gestational day 120. Decidual region shows increased colocalization of PKA and IGFBP-1 (indicated in yellow) in MNR (F) compared with control (C) in merged channel images. Negative controls (G and H). Nuclei are stained with DAPI (blue). Abbreviations: IGFBP-1, insulin-like growth factor-binding protein-1; PKA, protein kinase A; MNR, maternal nutrient reduction; DAPI, 4',6-diamidino-2-phenylindole.

phosphorylating decidual IGFBP-1. First, as shown by PRM-MS, PKA was co-IP with IGFBP-1 and activated in primary decidualized HESC in response to hypoxia. Second, using dual IF, we demonstrated that hypoxia caused increased expression and colocalization of PKA with IGFBP-1 in decidualized HESC. Dual IF combined with quantitative PLA provided strong evidence for a greater colocalization and potential interaction of PKA with IGFBP-1 in human IUGR. Importantly, this study used the baboon as a non-human primate model of MNR; we reported an increased PKA and IGFBP-1 colocalization and interaction of PKA with IGFBP-1 using PLA, 6 weeks before IUGR was observable. These data are consistent with the possibility that PKA phosphorylation of decidual IGFBP-1 precedes restricted fetal growth.

The ideal experimental paradigm to establish whether increased PKA coexpression and its association with IGFBP-1 occurs prior to the development of IUGR would be to conduct a time-course study in human pregnancy. However, due to limitations with such experimentation in women, we used a baboon

model of MNR associated with the development of IUGR in late pregnancy. Baboons (*Papio* spp.) share striking similarities with humans regarding placental structure, utero-placental blood flow, and fetal development.³² The similarities are also evident in the structure of the maternal-fetal barrier.³³ In addition, the discoid hemochorial placental structure and endocrine system are shared between the two species. Thus, studies of PKA and IGFBP-1 phosphorylation in the decidua of control and MNR baboon may provide insight into the regulation of decidual IGFBP-1 phosphorylation in women. Indeed, the findings in the non-human primate and human decidua were strikingly similar in the current study, supporting our overall conclusion.

Our previous work has demonstrated that human IUGR is associated with the activation of decidual CK2 and increased circulating levels of phosphorylated IGFBP-1.¹¹ In addition, involvement of PKC together with CK2 was reported in decidualized primary HESC cultured under hypoxic conditions.²⁹ Decidual IGFBP-1 regulates the bioavailability of IGF-1 within the local

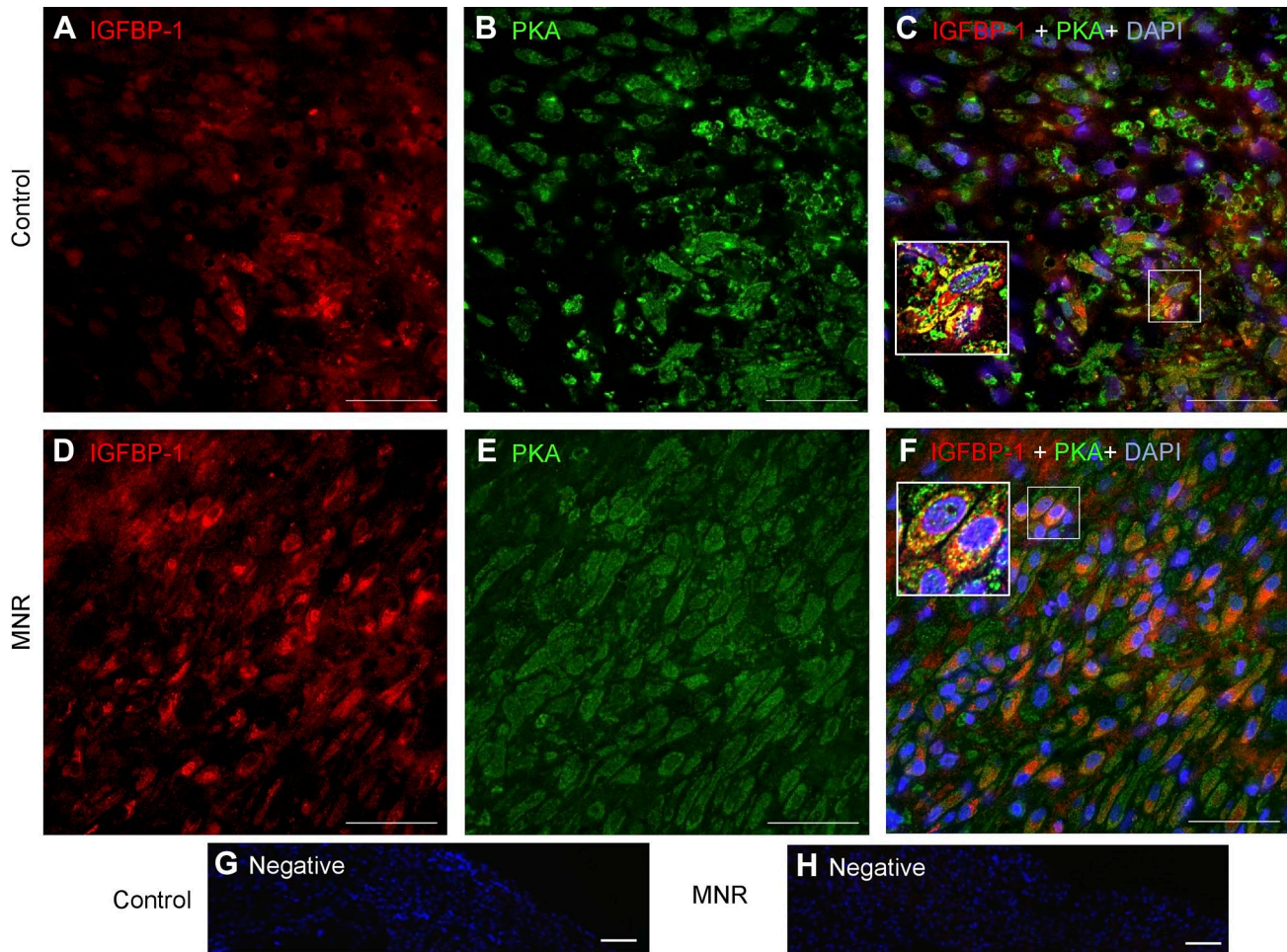


Figure 9. Increased decidual IGFBP-1 and PKA colocalization in MNR baboons at gestational day 120 as shown by deconvolution of images. Representative immunofluorescence staining of PKA (green) and IGFBP-1 (red) in the decidual region of control and MNR baboon placenta is shown by two-dimensional deconvolution of images. Single-channel IGFBP-1 (A and D) and PKA (B and E) are shown as multichannel (C) and (F) deconvolved images indicating colocalization of IGFBP-1 and PKA in the decidua of control and MNR baboons, with marked increase in areas of colocalization in the MNR decidua. Abbreviations: IGFBP-1, insulin-like growth factor-binding protein-1; PKA, protein kinase A; MNR, maternal nutrient reduction; DAPI, 4',6-diamidino-2-phenylindole; AGA, appropriate for gestational age.

environment of the placenta.¹ In the current study, we have not directly shown that PKA-mediated phosphorylation affects the affinity of IGFBP-1 to bind IGF-1 and hence IGF-1 bioavailability. However, we have previously demonstrated that increased IGFBP-1 phosphorylation leads to inhibition of IGF-1-induced IGF-1R autophosphorylation functionally, irrespective of the kinase involved.^{8,13,25,28,29} We therefore propose that the activation of decidual PKA as reported in the current study promotes interaction and phosphorylation of decidual IGFBP-1, which could lead to decreased IGF-1 bioavailability at the maternal–fetal interface early in pregnancy prior to development of IUGR.

The region of the decidua directly beneath the site of implantation forms the decidua basalis. The main

cell type of the decidua is decidualized endometrial stromal cells, which provide nutritional support and play an important functional role in pregnancy.³⁴ The major secretory products of decidual cells are prolactin (PRL) and IGFBP-1, which have been used widely as markers for decidualization.³⁵ Decidualized HESC secrete decidual-specific products such as PRL and IGFBP-1 and mimic the decidual microenvironment during normal pregnancy.³⁶ These literature data, together with our previous studies with decidualized HESC in vitro, suggest that HESC represent a relevant model of human decidual cells in vivo.^{21,22,25} Human IUGR is believed to be associated with some degree of placental hypoxia^{37,38} and we have previously reported markedly increased phosphorylation

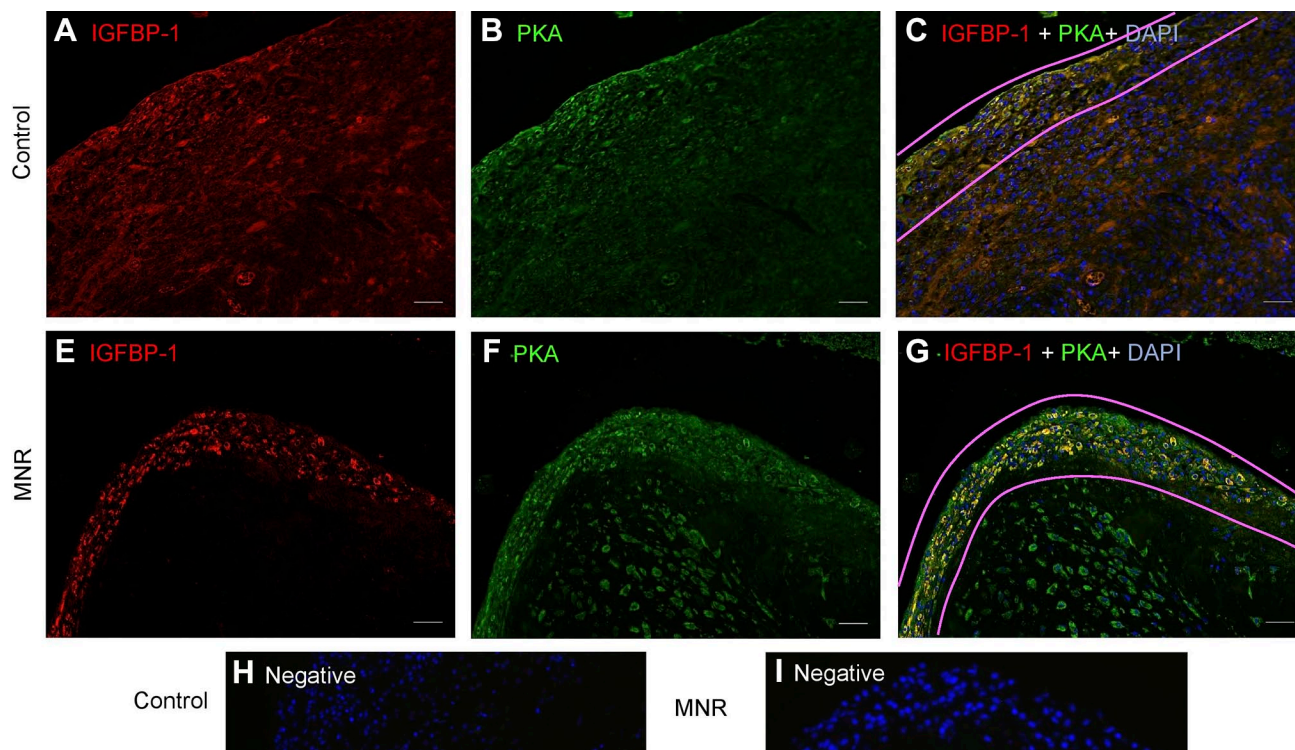


Figure 10. Increased decidual IGFBP-1 and PKA colocalization in MNR baboons at gestational day 165. Representative immunofluorescence staining of PKA (green) and IGFBP-1 (red) in the decidual region of control and MNR baboon placenta at gestational day 165. Decidual region shows increased colocalization of PKA and IGFBP-1 (indicated in yellow) in MNR (G) compared with control (C) in merged channel images. Negative controls (H and I). Nuclei are stained with DAPI (blue). Abbreviations: IGFBP-1, insulin-like growth factor binding protein-1; PKA, Protein kinase A; MNR, maternal nutrient reduction; DAPI, 4',6-diamidino-2-phenylindole; AGA, appropriate for gestational age.

of decidual IGFBP-1 in pregnancies complicated by IUGR.¹¹ In the current study, we show that IGFBP-1 phosphorylation is increased in response to hypoxia in HESC, providing a possible link between hypoxia and IGFBP-1 hyperphosphorylation in the IUGR decida.

The main strengths of this study are that we used highly appropriate and specific approaches. PRM-MS-based targeted protein quantification led to the acquisition of mass spectra of PKA and IGFBP-1 peptides with high resolution and mass accuracy. We identified multiple PKA-specific peptides ($n > 30$) that were co-IP with IGFBP-1. Furthermore, PRM-MS showed active PKA-pThr197 (autophosphorylation) along with a marked increase in IGFBP-1 phosphorylation at pSer169+174 along with pSer98+101 and pSer119 in hypoxia-treated decidualized HESC compared with normoxia. In addition, we used PLA, a highly specific, and sensitive immunohistochemical tool, to detect and quantify protein–protein interactions in situ (at distances < 40 nm) at endogenous protein levels.³⁹ Using PLA, we demonstrated a significant

increase in interaction between decidual PKA with IGFBP-1 in the human and baboon IUGR placenta. Data in the current study using PRM-MS and PLA along with standard dual IF in decidualized HESC and in human and baboon decida provided strong evidence that PKA interacts with IGFBP-1 in response to hypoxia and in IUGR. These data are consistent with the possibility that PKA is one of multiple kinases that mediates IGFBP-1 hyperphosphorylation in IUGR.

In the first trimester of pregnancy, extravillous trophoblast cells (EVTs) invade and transform decidual spiral arteries into low-resistance vessels.⁴⁰ During this process, IGFBP-1 has been shown to inhibit trophoblast invasion²⁰ by sequestering IGF-1.¹⁴ Decidual IGFBP-1 regulates the bioavailability of IGF-1 within the local environment of the placenta.²⁰ We propose that increased PKA-mediated phosphorylation of decidual IGFBP-1 contributes to a decreased IGF-1 bioavailability in the maternal–fetal interface in IUGR. Further studies are required to mechanistically link PKA to decidual IGFBP-1 hyperphosphorylation.

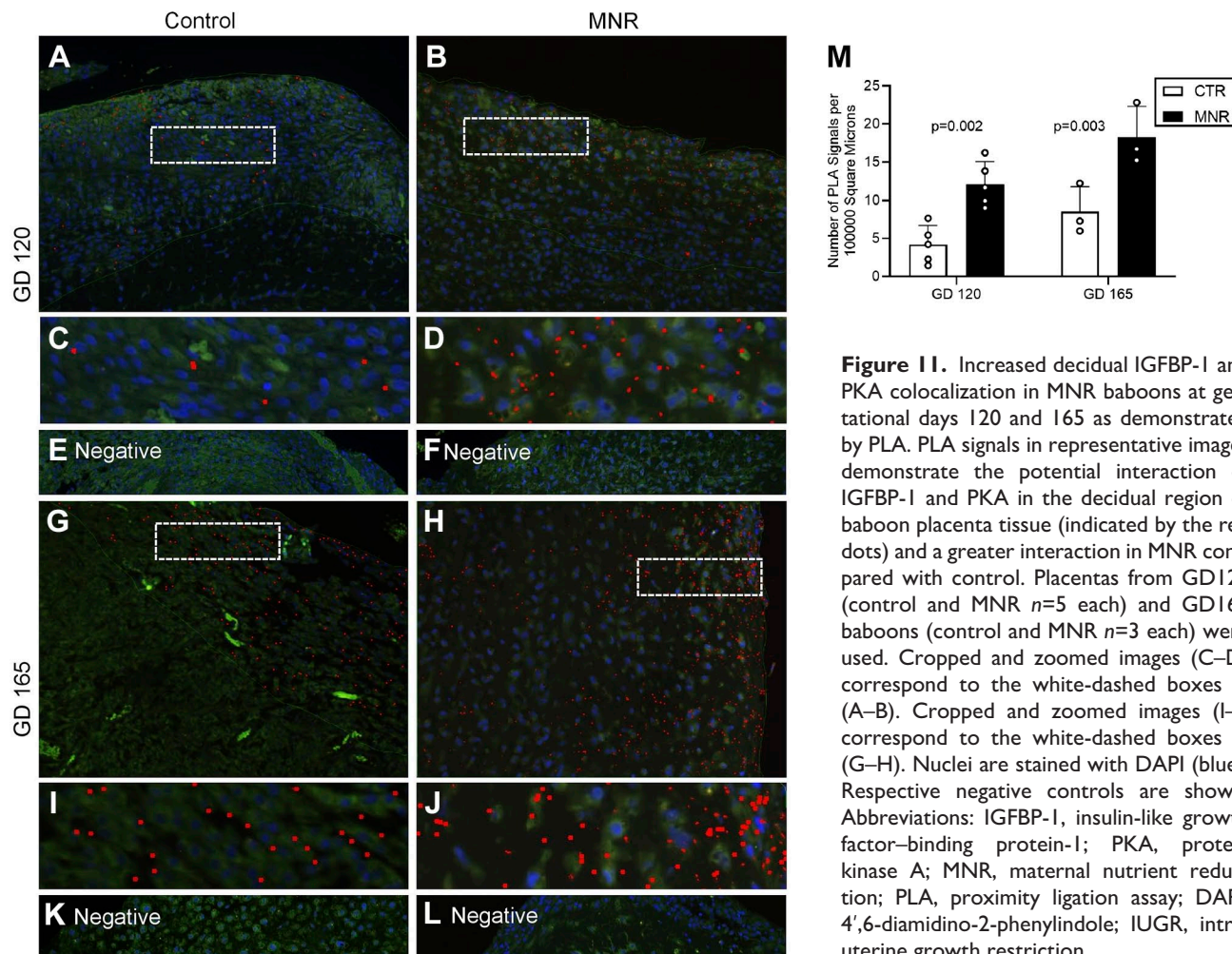


Figure 11. Increased decidual IGFBP-1 and PKA colocalization in MNR baboons at gestational days 120 and 165 as demonstrated by PLA. PLA signals in representative images demonstrate the potential interaction of IGFBP-1 and PKA in the decidual region of baboon placenta tissue (indicated by the red dots) and a greater interaction in MNR compared with control. Placentas from GD120 (control and MNR $n=5$ each) and GD165 baboons (control and MNR $n=3$ each) were used. Cropped and zoomed images (C–D) correspond to the white-dashed boxes in (A–B). Cropped and zoomed images (I–J) correspond to the white-dashed boxes in (G–H). Nuclei are stained with DAPI (blue). Respective negative controls are shown. Abbreviations: IGFBP-1, insulin-like growth factor-binding protein-1; PKA, protein kinase A; MNR, maternal nutrient reduction; PLA, proximity ligation assay; DAPI, 4',6-diamidino-2-phenylindole; IUGR, intrauterine growth restriction.

Acknowledgments

We thank Drs. Erin Lovett and Stephanie Black (Department of Obstetrics and Gynecology, University of Western Ontario, Canada) for their generous support in the collection of most valuable placenta tissue samples for this study. We thank Prof. Robert Baxter (Kolling Institute of Medical Research, University of Sydney, Sydney, Australia) for his kind gift of IGFBP-1 polyclonal antibody, and Biotron Integrated Microscopy, University of Western Ontario, in aiding immunohistochemistry, dual immunofluorescence, and PLA image acquisition and analyses.

Competing Interests

The author(s) declared no potential conflicts of interest with respect to the research, authorship, and/or publication of this article.

Author Contributions


TJ and MBG designed the research; KB performed the research; KB, MBG, and TJ analyzed and interpreted data;

TJ and MBG wrote the paper; KB wrote a draft of the paper; CL and PWN contributed new reagents and analytic tools and reviewed the paper. All authors reviewed and approved final version of the paper.

Funding

The author(s) disclosed receipt of the following financial support for the research, authorship, and/or publication of this article: This work was supported by grants from the National Institute of Health (HD089980 and HD078313 to M.B.G. and T.J. and HD021350 and AG057758 to P.W.N.).

ORCID iD

Peter W. Nathanielsz  <https://orcid.org/0000-0003-0802-0084>

Literature Cited

- Gibson JM, Aplin JD, White A, Westwood M. Regulation of IGF bioavailability in pregnancy. *Mol Hum Reprod.* 2001;7(1):79–87.

2. Clemmons DR. IGF binding proteins and their functions. *Mol Reprod Dev.* 1993;35(4):368–74.
3. Martina NA, Kim E, Chitkara U, Wathen NC, Chard T, Giudice LC. Gestational age-dependent expression of insulin-like growth factor-binding protein-1 (IGFBP-1) phosphoisoforms in human extraembryonic cavities, maternal serum, and decidua suggests decidua as the primary source of IGFBP-1 in these fluids during early pregnancy. *J Clin Endocrinol Metab.* 1997;82(6):1894–8.
4. Seferovic MD, Ali R, Kamei H, Liu S, Khosravi JM, Nazarian S, Han VK, Duan C, Gupta MB. Hypoxia and leucine deprivation induce human insulin-like growth factor binding protein-1 hyperphosphorylation and increase its biological activity. *Endocrinology.* 2009;150(1):220–31.
5. Westwood M, Gibson JM, Davies AJ, Young RJ, White A. The phosphorylation pattern of insulin-like growth factor-binding protein-1 in normal plasma is different from that in amniotic fluid and changes during pregnancy. *J Clin Endocrinol Metab.* 1994;79(6):1735–41.
6. Forbes K, Westwood M. The IGF axis and placental function. a mini review. *Horm Res.* 2008;69(3):129–37.
7. Crossey PA, Pillai CC, Miell JP. Altered placental development and intrauterine growth restriction in IGF binding protein-1 transgenic mice. *J Clin Invest.* 2002;110(3):411–8.
8. Abu Shehab M, Damerill I, Shen T, Rosario FJ, Nijland M, Nathanielsz PW, Kamat A, Jansson T, Gupta MB. Liver mTOR controls IGF-I bioavailability by regulation of protein kinase CK2 and IGFBP-1 phosphorylation in fetal growth restriction. *Endocrinology.* 2014;155(4):1327–39.
9. Singal SS, Nygard K, Dhruv MR, Biggar K, Shehab MA, Li SS, Jansson T, Gupta MB. Co-localization of insulin-like growth factor binding protein-1, casein kinase-2 β , and mechanistic target of rapamycin in Human hepatocellular carcinoma cells as demonstrated by dual immunofluorescence and in situ proximity ligation assay. *Am J Pathol.* 2018;188(1):111–24.
10. Chen AW, Biggar K, Nygard K, Singal S, Zhao T, Li C, Nathanielsz PW, Jansson T, Gupta MB. IGFBP-1 hyperphosphorylation in response to nutrient deprivation is mediated by activation of protein kinase C α (PKC α). *Mol Cell Endocrinol.* 2021;536:111400.
11. Gupta MB, Abu Shehab M, Nygard K, Biggar K, Singal SS, Santoro N, Powell TL, Jansson T. IUGR is associated with marked hyperphosphorylation of decidual and maternal plasma IGFBP-1. *J Clin Endocrinol Metab.* 2019;104(2):408–22.
12. Frost RA, Tseng L. Insulin-like growth factor-binding protein-1 is phosphorylated by cultured human endometrial stromal cells and multiple protein kinases in vitro. *J Biol Chem.* 1991;266(27):18082–8.
13. Malkani N, Biggar K, Shehab MA, Li SS, Jansson T, Gupta MB. Increased IGFBP-1 phosphorylation in response to leucine deprivation is mediated by CK2 and PKC. *Mol Cell Endocrinol.* 2016;425:48–60.
14. Asaoka Y. Chapter thirteen—phosphorylation of Gli by cAMP-dependent protein kinase. In: Litwack G, editor. *Vitamins & hormones.* Cambridge, MA: Academic Press; 2012. p. 293–307.
15. Gerbaud P, Taskén K, Pidoux G. Spatiotemporal regulation of cAMP signaling controls the human trophoblast fusion. *Front Pharmacol.* 2015;6:202.
16. Telgmann R, Maronde E, Taskén K, Gellersen B. Activated protein kinase A is required for differentiation-dependent transcription of the decidual prolactin gene in human endometrial stromal cells. *Endocrinology.* 1997;138(3):929–37.
17. Yee GM, Kennedy TG. Prostaglandin E2, cAMP and cAMP-dependent protein kinase isozymes during decidualization of rat endometrial stromal cells in vitro. *Prostaglandins.* 1993;46(2):117–38.
18. Peregrine E, Peebles D. Fetal growth and growth restriction. In: Rodeck CH, Whittle MJ editors. *Fetal medicine: basic science and clinical practice.* 2nd ed. St. Louis, MO: Elsevier; 2009. p. 541–58.
19. Reister F, Heyl W, Kaufmann P, Rath W. Trophoblast invasion in pre-eclampsia. *Zentralbl Gynakol.* 1999;121(12):587–90.
20. Irwin JC, Giudice LC. Insulin-like growth factor binding protein-1 binds to placental cytotrophoblast alpha5beta1 integrin and inhibits cytotrophoblast invasion into decidualized endometrial stromal cultures. *Growth Horm IGF Res.* 1998;8(1):21–31.
21. Chapdelaine P, Kang J, Boucher-Kovalik S, Caron N, Tremblay JP, Fortier MA. Decidualization and maintenance of a functional prostaglandin system in human endometrial cell lines following transformation with SV40 large T antigen. *Mol Hum Reprod.* 2006;12(5):309–19.
22. Krikun G, Mor G, Alvero A, Guller S, Schatz F, Sapi E, Rahman M, Caze R, Qumsiyeh M, Lockwood CJ. A novel immortalized human endometrial stromal cell line with normal progesterational response. *Endocrinology.* 2004;145(5):2291–6.
23. Logan PC, Steiner M, Ponnampalam AP, Mitchell MD. Cell cycle regulation of human endometrial stromal cells during decidualization. *Reprod Sci.* 2021;19(8):883–94.
24. Shehab MA, Biggar K, Singal SS, Nygard K, Shun-Cheng Li S, Jansson T, Gupta MB. Exposure of decidualized HIESC to low oxygen tension and leucine deprivation results in increased IGFBP-1 phosphorylation and reduced IGF-I bioactivity. *Mol Cell Endocrinol.* 2017;452:1–14.
25. Abu Shehab M, Biggar K, Kakadia JH, Dhruv M, Jain B, Nandi P, Nygard K, Jansson T, Gupta MB. Inhibition of decidual IGF-1 signaling in response to hypoxia and leucine deprivation is mediated by mTOR and AAR pathways and increased IGFBP-1 phosphorylation. *Mol Cell Endocrinol.* 2020;512:110865.
26. McDonald TJ, Wu G, Nijland MJ, Jenkins SL, Nathanielsz PW, Jansson T. Effect of 30% nutrient restriction in the first half of gestation on maternal and fetal baboon serum amino acid concentrations. *Br J Nutr.* 2013;109(8):1382–8.
27. Kakadia J, Biggar K, Jain B, Chen AW, Nygard K, Li C, Nathanielsz PW, Jansson T, Gupta MB. Mechanisms linking hypoxia to phosphorylation of insulin-like growth

- factor binding protein-1 in baboon fetuses with intra-uterine growth restriction and in cell culture. *Faseb J*. 2021;35(9):e21788.
28. Kakadia JH, Jain BB, Biggar K, Sutherland A, Nygard K, Li C, Nathanielsz PW, Jansson T, Gupta MB. Hyperphosphorylation of fetal liver IGFBP-1 precedes slowing of fetal growth in nutrient-restricted baboons and may be a mechanism underlying IUGR. *Am J Physiol Endocrinol Metab*. 2020;319(3):E614–28.
 29. Nandi P, Jang CE, Biggar K, Halari CD, Jansson T, Gupta MB. Mechanistic target of rapamycin complex 1 signaling links hypoxia to increased IGFBP-1 phosphorylation in primary human decidualized endometrial stromal cells. *Biomolecules*. 2021;11(9):1382.
 30. Singal SS, Nygard K, Gratton R, Jansson T, Gupta MB. Increased insulin-like growth factor binding protein-1 phosphorylation in decidualized stromal mesenchymal cells in human intrauterine growth restriction placentas. *J Histochem Cytochem*. 2018;66(9):617–30.
 31. Franke WW, Schmid E, Osborn M, Weber K. Different intermediate-sized filaments distinguished by immunofluorescence microscopy. *Proc Natl Acad Sci USA*. 1978;75(10):5034–8.
 32. Schenone MH, Schlabritz-Loutsevitch N, Zhang J, Samson JE, Mari G, Ferry RJ, Hubbard GB, Dick EJ. Abruptio placentae in the baboon (*Papio spp.*). *Placenta*. 2012;33(4):278–84.
 33. Samson JE, Mari G, Dick EJ, Hubbard GB, Ferry RJ, Schlabritz-Loutsevitch NE. The morphometry of materno-fetal oxygen exchange barrier in a baboon model of obesity. *Placenta*. 2011;32(11):845–51.
 34. Su RW, Fazleabas AT. Implantation and establishment of pregnancy in human and nonhuman primates. *Adv Anat Embryol Cell Biol*. 2015;216:189–213.
 35. Gellersen B, Brosens IA, Brosens JJ. Decidualization of the human endometrium: mechanisms, functions, and clinical perspectives. *Semin Reprod Med*. 2007;25(6):445–53.
 36. Richards RG, Brar AK, Frank GR, Hartman SM, Jikihara H. Fibroblast cells from term human decidua closely resemble endometrial stromal cells: induction of prolactin and insulin-like growth factor binding protein-1 expression. *Biol Reprod*. 1995;52(3):609–15.
 37. Seferovic MD, Gupta MB. Increased umbilical cord PAI-1 levels in placental insufficiency are associated with fetal hypoxia and angiogenesis. *Dis Markers*. 2016; 2016:7124186.
 38. van Patot MC, Bensperger G, Gassmann M, Llanos AJ. The hypoxic placenta. *High Alt Med Biol*. 2012; 13(3):176–84.
 39. Gullberg M, Andersson AC. Visualization and quantification of protein-protein interactions in cells and tissues. *Nat Methods*. 2010;7(6):v–vi.
 40. Moser G, Weiss G, Sundl M, Gauster M, Siwetz M, Lang-Olip I, Huppertz B. Extravillous trophoblasts invade more than uterine arteries: evidence for the invasion of uterine veins. *Histochem Cell Biol*. 2017;147(3): 353–66.